Novel tunneling technique for measuring electron scattering rates in superconductors: Application to Sn and Sn-In films

Yeouchung Yen* and Thomas R. Lemberger
Department of Physics, Ohio State University, Columbus, Ohio 43210
(Received 12 August 1987)

The low-voltage resistances $R_j(T,I_s)$ of low-resistance Sn/Sn-oxide/Cu and $Sn_{0.95}In_{0.05}$/Sn-In-oxide/Cu tunnel junctions were measured as functions of temperature and supercurrent along the Sn or Sn-In film. From precise numerical fits to a recent theory, we determined the electron-phonon scattering rate at T_c for both Sn and Sn-In to be $\tau_{e-ph}(T_c)^{-1}\approx 2.8\times 10^9 s^{-1}\pm 10\%$, with the assumption of an electron-phonon coupling $\alpha^2F(\omega)\propto\omega^2$. We determined that the crystalline anisotropy of the order parameter Δ was proportional to electron mean free path squared, as expected theoretically. Extrapolation to infinite mean free path gave a value for the mean-square anisotropy in Δ in pure Sn of $\langle a^2\rangle_0=0.0053\pm 13\%$. The consistency of these results from sample to sample, and the agreement between all of these results and published theoretical and experimental work, verifies the theory and demonstrates the feasibility of using such measurements to study electron scattering in novel superconducting materials.

I. INTRODUCTION

A recent theory describes how measurements of the low-voltage resistance of low-resistance superconductor/insulator/normal-metal ($S/I/N$) tunnel junctions might be used to study pair-breaking electron-scattering mechanisms in superconducting films.[1] The results presented here verify the theory and demonstrate the feasibility of further applications of the method.

According to the theory, the resistance is to be measured[2-6] as a function of temperature and supercurrent in the S film. The junctions should have such low resistances that the quasiparticle charge imbalance[7] generated by the measuring current contributes measurably to the junction resistance. A particularly important feature which distinguishes the theory from earlier work is the inclusion of the proximity-effect[8-10] coupling between the S and N films through the insulator, which leads to a "tunneling" charge-imbalance relaxation process in addition to "bulk" processes such as electron-phonon scattering.

The primary motivation, and result, of our measurements on Sn and Sn-In films is to validate the theory on a material that is reasonably well understood but more difficult to work with than, e.g., Al, and thereby demonstrate the feasibility of using similar measurements and analysis to study less-well-understood materials.

The basic effects of a quasiparticle disequilibrium, i.e., charge imbalance, on the resistance of a $S/I/N$ junction are the following. A nonequilibrium state is generated in a superconductor as a current flows through a low-resistance $S/I/N$ tunnel junction. This nonequilibrium state, referred to as charge imbalance Q^* in the literature,[1-8,11-30] has an unequal density of electronlike ($k>k_f$) and holelike ($k<k_f$) excitations. Q^* results in a shift in the condensate chemical potential. This causes the electrochemical potential difference between S and N in the presence of Q^* to be larger than the electrostatic potential alone. For a given current, this extra voltage is interpreted experimentally as an extra "nonequilibrium" resistance $R_{Q^*}(T)$ in addition to the "equilibrium" resistance associated with the electrostatic potential across the junction oxide barrier. The size and temperature dependence of $R_{Q^*}(T)$ are very sensitive to pair-breaking mechanisms that are intrinsic or extrinsic to the superconductor since pair breakers increase the Q^* relaxation rate and therefore reduce Q^* and the nonequilibrium component of the junction resistance.

A transport supercurrent serves as a pair breaker[31] and relaxes Q^* (Ref. 17) because it makes the order parameter anisotropic which makes elastic scattering from defects pair breaking. The pair-breaking rate associated with a supercurrent depends explicitly on temperature and on the energy of the scattered quasiparticle. This temperature and energy dependence of the pair-breaking rate, together with those of the intrinsic pair breakers, are reflected in the dependence of junction resistance on supercurrent. From a detailed numerical fit to the data one can obtain information on the magnitude, as well as the energy and temperature dependence of the scattering mechanisms that are intrinsic to the superconductor.

Other nonequilibrium techniques involving charge imbalance[7,11-19] have been used to study electron scattering in superconductors.[7] Clarke[11] first used a three-film, two-junction geometry to measure the shift in the chemical potential associated with Q^* as a result of tunnel injection of quasiparticles. Subsequently, Clarke and Paterson[12] verified qualitatively that elastic scattering with an anisotropic order parameter[32] could also relax Q^*. Chi and Clarke[14] then deduced an average value of intrinsic gap-anisotropy parameter $\langle a^2\rangle_0$ from the dependence of $\tau_{Q^*}^{-1}$ on Δ/k_BT_c on Al films with various electron mean free paths. Hsiang and Clarke[15] looked at the boundary resistance of Sn/Ir/Sn $S/N/S$ interfaces and obtained an

electron-phonon rate from their fit. Lemberger and Clarke[16,17] measured the charge-imbalance relaxation rate as a function of magnetic-impurity concentration and as a function of applied supercurrent. While none of these earlier charge-imbalance studies obtained the detailed agreement between theory and experiment obtained in the present study, they are the foundation upon which the present work is built.

The theoretical understanding[4,8,20–30] of charge imbalance proceeded parallel to the experimental developments. Tinkham[21] first considered charge relaxation due to inelastic electron-phonon scattering and elastic scattering with intrinsic gap anisotropy. Tinkham's theory was extended by several authors[22–25,28–30] to more rigorous treatment and to include other relaxation mechanisms. Schmid and Schön[22] and Pethick and Smith[25,28] using Green's functions and a Boltzmann-equation approach, respectively, showed how to include charge-imbalance relaxation from magnetic impurities, a magnetic field, or an applied supercurrent. In regard to measurements on the double-junction configuration, which is most closely related to the present measurements, the theory described the data reasonably well near T_c, but showed significant deviations below roughly $0.95T_c$. In an effort to improve agreement, the theory was extended to describe a simpler physical situation, namely a single $S/I/N$ junction, with the inclusion of the proximity coupling between the S and N films.[1]

In this paper, we report measurements of the low-voltage resistance of low-resistance Sn/Sn-oxide/Cu and Sn-In/Sn-In–oxide/Cu tunnel junctions as functions of temperature and transport supercurrent. Our major quantitative results are the electron-phonon scattering rate at the Fermi surface at T_c, $\tau_{e\text{-ph}}(T_c)^{-1}$, and the mean-square intrinsic gap anisotropy, $\langle a^2\rangle_0$, for pure Sn, extrapolated from films with a short electron mean free path.

The organization of the paper is as follows. In Sec. II we describe the theory. In particular, we discuss the effect of intrinsic gap anisotropy on charge-imbalance relaxation. Section III gives the relevant experimental details. Section IV contains the experimental results and discussions, followed by our conclusions in Sec. V.

II. THEORETICAL BACKGROUND

The theoretical background for extracting information on electron-scattering mechanisms from measurements of the low-voltage resistance of a superconductor/insulator/normal-metal ($S/I/N$) tunnel junction has been discussed in detail in Ref. 1. For clarity and simplicity, Ref. 1 left out the effect of intrinsic gap anisotropy in the relaxation of charge imbalance. In this section we summarize the salient points of Ref. 1 and discuss the effect of intrinsic gap anisotropy on charge-imbalance relaxation.

An important concept in the theory is that there is a proximity-effect-induced[9,10] charge-imbalance relaxation mechanism associated with a $S/I/N$ tunnel junction whereby excess quasiparticles relax by tunneling back from the S electrode into the N electrode. This backflow results in a net electric current opposed to the total current. The total current flowing through the junction is the difference between a forward equilibrium current proportional to the electrostatic potential $[V-Q^*/2N(0)|e|]$ and a reverse nonequilibrium current proportional to the chemical-potential drop $Q^*/2N(0)|e|$ across the junction due to the charge imbalance. Here $2N(0)$ is the normal-state density of states, e is the electronic charge, and Q^* is the net quasiparticle electron density. The physical meaning of this separation of current is that the electrostatic potential is the applied perturbation to the system and the chemical potential shift is the response of the system to the perturbation.

In analogy to separation of the total current, one should also regard the total quasiparticle injection rate as the difference between the equilibrium and nonequilibrium components corresponding to the applied perturbation and the system response. There is a different between the total current I and the total quasiparticle injection rate. Only a fraction F^* of the equilibrium current goes into the superconductor as quasiparticle charge, the rest of the current goes directly into the condensate. F^* is unity at T_c and decreases monotonically towards lower temperatures.[27]

The resistance of the junction is obtained by expressing Q^* in terms of F^*, g_{NS}, τ_{tun}, and the charge-imbalance relaxation time τ_{Q^*} in the expression for the total current I. From Eqs. (27)–(29) of Ref. 1 we have

$$R_j(T)=R_{\text{eq}}(T)+R_{Q^*}(T)\ , \tag{1}$$

$$R_{\text{eq}}(T)=R_N/g_{NS}(T)\ , \tag{2}$$

$$R_{Q^*}(T)=R_{\text{eq}}(T)/[\tau_{\text{tun}}/F^*\tau_{Q^*}-(1-g_{NS})]\ . \tag{3}$$

Equation (1) shows that the total junction resistance $R_j(T)$ consists of the equilibrium part $R_{\text{eq}}(T)$ and the nonequilibrium part $R_{Q^*}(T)$. $g_{NS}(T)$ is the conductance of the junction in the absence of nonequilibrium effects, normalized to its value at T_c. It has been tabulated by Bermon.[33] R_N is the intrinsic resistance of the junction so that $R_{\text{eq}}(T)$ is just the junction resistance when there is no charge imbalance. τ_{tun}^{-1} is the proximity-effect-induced tunneling rate[4–6,8] defined by

$$\tau_{\text{tun}}^{-1}=[2N(0)e^2\Omega R_N]^{-1}\ , \tag{4}$$

where Ω is the volume of the nonequilibrium region. As expected, the nonequilibrium part of the junction resistance depends on τ_{tun}^{-1} and $\tau_{Q^*}^{-1}$.

The charge-imbalance relaxation rate $\tau_{Q^*}^{-1}$ is determined by all the scattering mechanisms in the superconductor under study. For the Sn and Sn-In films we report in this paper, the important scattering mechanisms are inelastic electron-phonon scattering,[1,21–23,25,26] proximity-effect-induced tunneling[4–6,8] and elastic scattering in the presence of intrinsic gap anisotropy. The first two processes have been discussed extensively by several authors and will not be discussed again here. Charge-imbalance relaxation in the presence of intrinsic gap anisotropy has been discussed by Chi and Clarke[14] in regard to its effect on double-junction studies. We give in the following details of gap-anisotropy effects on the

resistance of a $S/I/N$ junction.

The intrinsic gap anisotropy affects the transition temperature of the superconductor since the effective phonon-mediated electron-electron interaction depends on the relative direction of electron momentum and the crystal axes.[34,35] The superconductor takes advantage of the existence of gap anisotropy in forming pairs and obtaining the highest T_c possible. Elastic scattering reduces the anisotropy and T_c.

The term in the Boltzman equation that describes elastic scattering of quasiparticles across the Fermi surface has the following form:[8,12,14]

$$G_{\rm el}(E)=\frac{1}{\tau_1}C_{\rm cf}N_1(E)(2\delta f_E)\ . \tag{5}$$

τ_1^{-1} is the elastic scattering rate in the normal state. C_{cf} is the coherence factor for this process. $N_1(E)$ is the superconducting tunneling density of states. δf_E is the deviation of the distribution function from its equilibrium value.

The coherence factor $C_{\rm cf}=(uu'-vv')^2$ is nonzero only when the gap is anisotropic.[21] Using the definitions of u and v,[36] the coherence factor for this process can be written

$$(uu'-vv')^2=\frac{\langle\Delta\rangle^2}{2\varepsilon^2}\langle a^2\rangle\ , \tag{6}$$

where

$$\langle a^2\rangle=\frac{\langle(\Delta-\langle\Delta\rangle)^2\rangle}{\langle\Delta\rangle^2} \tag{7}$$

is averaged over the Fermi surface. Combining Eqs. (5) and (6) we have

$$G_{\rm el}(E)=\frac{\langle a^2\rangle}{2\tau_1}\frac{\langle\Delta\rangle^2}{\varepsilon^2}N_1(E)(2\delta f_E)\ , \tag{8}$$

where $\langle a^2\rangle/2\tau_1$ is the characteristic rate for intrinsic gap anisotropy scattering. For simplicity, we replace $\langle\Delta\rangle$ with Δ in the rest of this paper.

In most superconductors, gap anisotropy suffers from Anderson[35] averaging when the electron mean free path is shortened by the addition of nonmagnetic impurities or by the existence of boundaries in thin films. The basic idea behind this is that elastic scattering mixes different momentum states from all directions and positions on the Fermi surface. As the electrons are scattered, they carry information of the Fermi surface from one place to the other. The end result is that the gap anisotropy is "averaged out." The characteristic rates to enter this averaging should then be the elastic scattering rate τ_1^{-1} and the gap rate $\Delta/\hbar$.

The degree of reduction in gap anisotropy due to this averaging is unclear from Anderson's original theory.[35] From the work of Markowitz and Kadanoff[34] on the behavior of Δ near T_c, Tinkham[21,37,38] assumed the averaged gap-anisotropy parameter to be

$$\langle a^2\rangle=\langle a^2\rangle_0/[1+(\hbar/2\tau_1\Delta)^2] \tag{9}$$

$$\approx 4\langle a^2\rangle_0\tau_1^2\Delta^2/\hbar^2\ , \tag{10}$$

where $\langle a^2\rangle_0$ is the intrinsic gap anisotropy parameter commonly used in the literature for a bulk clean superconductor. The factor $(\hbar^2/2\tau_1\Delta)^2$ is very large for our Sn-In films, typically about 100–1000, so that one can rewrite Eq. (9) as Eq. (10). Note that $\langle a^2\rangle$ increases as the temperature decreases since Δ increases as the temperature decreases.

Combining Eqs. (5), (6), and (10) for $(\hbar^2/2\tau_1\Delta)^2\gg 1$, we have

$$G_{\rm el}(E)=\tau_{\rm qel0}^{-1}\frac{\Delta^2}{(k_BT_c)^2}\frac{\Delta^2}{\varepsilon^2}N_1(E)(2\delta f_E)\ , \tag{11}$$

where

$$\tau_{\rm qel0}^{-1}=\frac{2\langle a^2\rangle_0\tau_1(k_BT_c)^2}{\hbar^2} \tag{12}$$

is the characteristic rate for intrinsic gap-anisotropy scattering in the dirty limit used by Chi and Clarke.[14] This characteristic rate is temperature independent and is proportional to the elastic scattering time τ_1 instead of the elastic scattering rate τ_1^{-1} because of the strong elastic scattering tending to make the order parameter Δ isotropic. The rate is proportional to $\langle a^2\rangle_0$ as expected. Since our pure Sn films do not satisfy $(\hbar^2/2\tau_1\Delta)^2\gg 1$ at low temperatures, we use Eqs. (8) and (9) in our calculations. Using Eqs. (11) and (12) results in a good fit to the pure Sn data, but with a value of $\langle a^2\rangle_0$ 20% smaller.

The product of the coherence factor and the tunneling density of states determines the energy dependence of the effective scattering rate as can be seen from Eq. (5). The intrinsic gap-anisotropy scattering rate is apparently largest for quasiparticles near the gap edge where both quantities are largest. That is, low-energy quasiparticles are more likely to scatter elastically across the Fermi surface. High-energy quasiparticles have to lower their energies by inelastic scattering before they can scatter elastically across the Fermi surface.

The temperature dependence of the scattering rate comes from the energy dependence of $C_{\rm cf}$ and $N_1(E)$ as well as the temperature dependence of Δ. To see this better, assume that all quasiparticles contributing to the scattering rate have an energy of $\Delta+k_BT$, as appropriate for a thermal distribution. At high temperatures, Δ is small and the product of $C_{\rm cf}N_1(E)$ is small at $E=\Delta+k_BT$. At low temperatures, Δ is large and so is the product of $C_{\rm cf}$ and $N_1(E)$. The gap-anisotropy rate may start with a value 10 times smaller than the electron-phonon rate at, say, $0.95T_c$ and be the dominant relaxation rate at low temperatures as the inelastic electron-phonon rate is frozen out. We emphasize that although the rate is largest at low temperatures, the strongest temperature dependence of this rate occurs at high temperatures. As we will see later in our data analysis, this allows us to determine the pair-breaking scattering rate due to intrinsic gap anisotropy from data taken at relatively high temperatures.

The effect of a transport supercurrent on charge-imbalance relaxation has been discussed in Refs. 1 and 17. From Eqs. (3)–(6) of Ref. 2, the pair-breaking rate

τ_s^{-1} can be written in terms of measurable quantities and the density of superconducting electrons, n_s:

$$\tau_s^{-1}=\frac{0.1669k_BT_c}{\hbar}\frac{n_s(0,0)^2}{n_s(T,\tau_s^{-1})^2}\frac{I_s^2}{I_c(0)^2}\ , \tag{13}$$

where

$$I_c(0)^2=\frac{2.562\,2N(0)d^2w^2(k_BT_c)^3}{\hbar\rho} \tag{14}$$

is the theoretical zero-temperature critical current.[39,40] d and w are the thickness and the width of the superconducting film, respectively. ρ is the resistivity of the S film at 4.2 K.

We point out that the entire temperature dependence of τ_s^{-1} is in that of $n_s(T,\tau_s^{-1})$ for a fixed current I_s. $n_s(T,\tau_s^{-1}=0)$ increases monotonically from zero at T_c to $mc^2/[4\pi\lambda(0)^2e^2]$ at $T=0$. $\lambda(0)$ is the zero-temperature penetration depth. In our analysis, we use the dirty-limit theory[31] to calculate $n_s(T)$.

The computer programs used in this study are the same as the ones used in Ref. 1 except that the effects of intrinsic gap anisotropy are included. Since the pair-breaking rate due to the intrinsic gap anisotropy depends on the order parameter itself, we iterated the calculation of Δ until a self-consistent set of gap-anisotropy pair-breaking rate and the order parameter were found. Because the rates were so small, this procedure had only a minor effect on the results. Checks on the program can be found in the Appendix of Ref. 1.

We now discuss resistance as a function of temperature and transport supercurrent. The resistance of the junction is composed of the equilibrium part $R_{\rm eq}(T)$ and the nonequilibrium part $R_{Q^*}(T)$. The resistance of the junction diverges towards T_c since R_{Q^*} diverges at T_c. $R_{\rm eq}(T)$ diverges towards low temperature since quasiparticles are thermally excited and therefore the junction resistance depends exponentially on Δ/k_BT at low temperature. Thus, $R_j(T)$ has a minimum around $0.9T_c$.

Both $R_{\rm eq}$ and R_{Q^*} are reduced by an applied transport supercurrent. The normalized reduction in the equilibrium part of the junction resistance, $-\delta R_{\rm eq}(T,I_s)/R_{\rm eq}(T,I_s=0)$, in the presence of a transport supercurrent has been investigated both theoretically and experimentally in high-resistance junctions where the nonequilibrium resistance is negligible, and excellent quantitative agreement was found.[2] Therefore, we are confident that we can calculate the pair-breaking rate $1/\tau_s$ accurately from the measured supercurrent I_s.

The reduction in the nonequilibrium part of the junction resistance by a supercurrent comes from the increase in the charge-imbalance relaxation rate. The effect is illustrated in Fig. 1 which shows the normalized reduction in the nonequilibrium part of the junction resistance $-\delta R_{Q^*}(T,I_s)/R_j(T,I_s=0)$ versus normalized supercurrent squared $I_s(T)^2/I_c(0)^2$ for two different gap-anisotropy rates at three different normalized temperatures. One can see that, at the same normalized temperature, the sizes of the effect are quite different for different gap-anisotropy rates. The size of the effect also depends strongly on the temperature given the same supercurrent and gap-anisotropy rate.

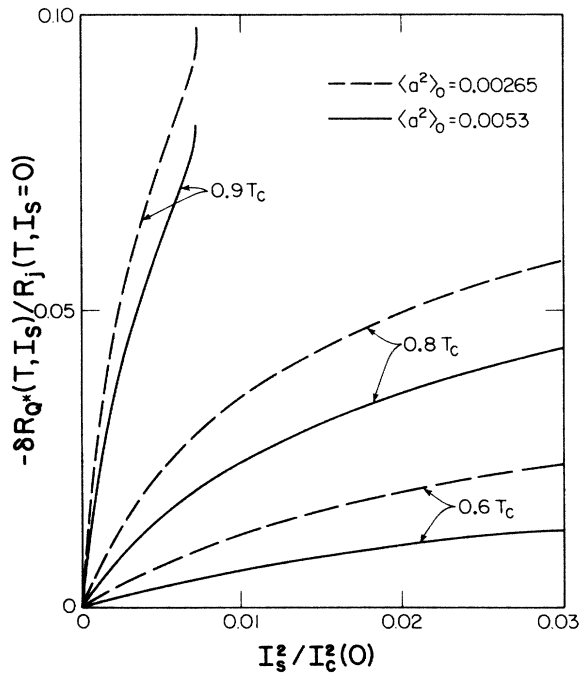

FIG. 1. Calculated reduction of the charge-imbalance part of the junction resistance (normalized to the junction resistance when there is no supercurrent), $-\delta R_{Q^*}(T,I_s)/R_j(T,I_S=0)$, vs the normalized supercurrent squared, $I_s(T)^2/I_c(0)^2$, for $\langle a^2\rangle_0$ of 0.0053 and 0.002 65 at $0.9T_c$, $0.8T_c$, and $0.6T_c$. At the same normalized temperature, gap anisotropy has an important effect on the size of the reduction. Given the same $\langle a^2\rangle_0$, the effect is strongly temperature dependent.

The resistance of the junction that one measures is the total junction resistance $R_j(T,I_s)$. The slope of the initial reduction in the junction resistance depends on the relative importance of changes in the equilibrium and nonequilibrium components. Near T_c, the charge-imbalance component dominates the change since the application of supercurrent greatly increases the charge-imbalance relaxation rate. The change in the density of states does not affect the junction resistance a great deal because most of the change in the density of states occurs near the gap edge while quasiparticles populate states of higher energies. At lower temperatures, the reduction in the equilibrium component becomes more and more important while the nonequilibrium component dies out due to the existence of intrinsic gap anisotropy. In actual data analysis, the temperature dependence of the slopes for the initial reduction serves as a check for the correct ratio of scattering rates involved while the size of the reduction in junction resistance ensures the correct choice of the magnitudes of scattering rates.

III. EXPERIMENTAL PROCEDURES

The samples were Sn/Sn-oxide/Cu or Sn-In/Sn-In-oxide/Cu tunnel junctions. The experimental pro-

cedure for making high-resistance Sn/Sn-oxide/Cu junctions has been reported elsewhere.[2] Here we describe the fabrication of low-resistance Sn/Sn-oxide/Cu and Sn-In/Sn-In-oxide/Cu junctions.

All of our films were deposited from resistively heated sources through mechanical masks onto glass substrates. To improve the uniformity of current distribution, samples were always built on substrates with ~5000-Å-thick Nb ground planes. These ground planes were anodized and then coated with ~2000 Å of SiO for insulation before use. The resistance between the samples and the Nb ground plane was always larger than 20 MΩ.

Figure 2 shows the sample geometry. The Sn and Sn-In films were normally 800 Å thick, the Cu-Al-Fe films were 2000–3000 Å thick, while the Pb overlayers were usually 2000 Å thick. SiO (~1500 Å) was used to define the area of the junctions to be $\sim 300 \times 300\ \mu m^2$.

For Sn/Sn-oxide/Cu junctions, 99.999%-pure Sn was first deposited onto a previously cleaned glass substrate through an aperture mask at a rate of 20–30 Å/s in a pressure of less than 10^{-6} torr. The substrate was held at −65 to −80 °C during evaporation using a cold finger. It was found that this substrate temperature range yielded the highest-quality Sn and Sn-In films. It was also found that the SiO underlayer used for insulating the Nb plane from the Sn film is important in obtaining high-quality films. The substrate was warmed to room temperature before the film was oxidized.

Several methods have been developed for oxidation of films. Each is suitable for different strengths of oxide barriers. We found for low-resistance junctions, oxidation in a reduced oxygen atmosphere (~2–10 mm Hg) for ~2 h gave junctions of highest quality.

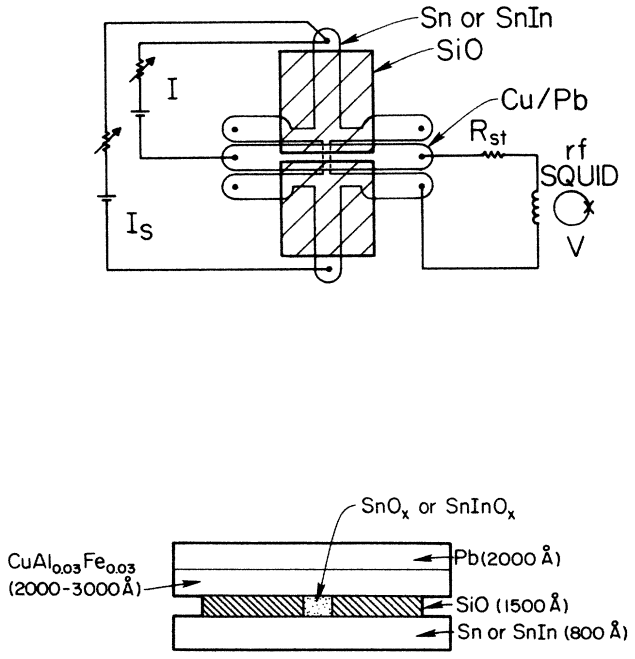

FIG. 2. Sample configuration: plan (top), side (bottom). I and V are the current and voltage in the junction; I_s is the supercurrent in the superconducting strip. For simplicity the Nb ground plane is not shown here. For the Sn sample a ~0.2-Ω wire was connected in parallel with the narrow part of the S film so that most current flows through the 0.2-Ω short when the critical current is exceeded.

After oxidizing the base film, the area of the junctions were defined by depositing SiO to mask off all but 300 μm of the narrow part of the base films. The substrate was then cooled to about −10 to −20 °C before counterelectrode deposition. A mixture of Cu, Al (3 wt. %), and Fe (3 wt. %) was deposited in 2×10^{-4}-torr O_2 to finish the tunnel junctions. The addition of Al and Fe, as well as evaporation in O_2, shortened the electron mean free path and the normal-state coherence length in the Cu, thus preventing a supercurrent from flowing from Sn to the Pb overlayer. It was essential to keep the substrate cold during deposition of the Cu mixture to avoid wetting of Cu by Sn.[41] The Pb overlayer was deposited to reduce the series resistance presented by the normal-metal strip to the SQUID (superconducting quantum-interference device) voltmeter. This was of great importance since the junction resistance could be as low as 40 μΩ and any series resistance in the circuit would impair the resolution of the measurements. The samples were then covered with SiO to protect them from recrystallization due to exposure to moisture in the air.

In the case of Sn-In/Sn-In-oxide/Cu junctions the initial procedure was slightly different. Instead of depositing 800 Å of Sn at one time we deposited in sequence 360 Å of Sn (at ~20–30 Å/s), 40 Å of In (at 4 Å/s), and 400 Å of Sn onto a cooled substrate, as for Sn films. The com- pleted film stayed in high vacuum (10^{-6} torr) for at least 1 h after it was warmed up to room temperature so that interdiffusion between Sn and In was completed.[42,43] The rest of the sample-preparation procedures were the same as those for Sn/Sn-oxide/Cu junction. It is well known that Sn and In interdiffuse quickly at room temperature provided proper high vacuum is maintained.[43] The resistivity of the completed Sn-In alloy films remained unchanged after the films were left at room temperature for more than 1 d, suggesting completion of interdiffusion. The apparent difference in the electron mean free path, as can be seen from Table I, gives additional support of complete interdiffusion.

We have found that a thin SiO overlayer on thin-film Sn affects the properties of Sn films even at 4.2 K. To avoid this problem we always measured strip properties with a bare Sn film which was deposited at the same time the base films for the junctions were deposited. Properties of Sn films in the junctions were not affected by SiO since they were only in contract with either a thicker SiO layer or the normal-metal counterelectrode. We observed that a thick layer of SiO (≥1500 Å) did not affect the properties of Sn films.

We attached wires to the samples using In pads to enable us to perform four-terminal measurements on R_s, R_j, and R_j versus I_s as functions of temperature. The In pads were far away from the narrow part of the strip so that no unwanted alloying effect occurred. This is supported by the film resistivity measurements. Figure 2 shows the wiring diagram. We connected a manganin wire of about 0.2 Ω in parallel with the Sn or Sn-In film so that most of the current passed through this low-

TABLE I. Material and sample parameters. Samples discussed in the text show a larger rise in resistance at low T than the rest of the samples that are listed here. See Ref. 45 for complete data.

S-film	Material	T_c (K)	$\rho_{4.2}$ (nΩ m)	l^a (nm)	w (μm)	w_{SiO} (μm)	d^b (nm)	$I_c(0)^c$ (A)	$R_N{}^d$ ($\mu\Omega$)	τ_{tun}^{-1} (10^9 s^{-1})	$\tau_{e\text{-ph}}(T_c)^{-1}$ (10^9 s^{-1})	$\langle a^2\rangle_0$
D20	Sn	3.72	5.63	187	254	385	80	6.06	26.0	1.18	2.78	0.0056
D26	Sn	3.72	6.58	160	254	346	80	5.98	40.4	0.79	2.80	0.0057
D30	Sn	3.72	5.73	183	244	385	80	6.16	39.4	0.76	2.86	0.0053
A13	Sn-In	3.69	28.0	37.5	280	323	80	3.48	47.0	0.60	3.00	0.0046
S28	Sn-In	3.68	29.3	35.8	297	330	80	3.44	85.5	0.32	2.47	0.0053

[a]Determined by using $\rho_{4.2}l = 1.05\times10^{-15}$ Ω m^2.
[b]Reading from a crystal-thickness monitor.
[c]Calculated from Eq. (14) with measured sample parameters.
[d]Determined from Eq. (4) with measured sample dimensions.

resistance path when the critical current of the superconducting film was exceeded. This is very important since the normal-state resistance of the Sn or Sn-In strip was about 1–3 Ω while the experimental critical current could be more than half an ampere. As a result, films which did not have a low-resistance short in parallel burned out once the critical current was exceeded.

The samples were mounted in a double-can probe with both cans coated with superconducting solder. A superconducting Pb bag was used to further reduce external magnetic fluctuations. Usually the system took about 3 h to reach 77 K starting from room temperature. The whole probe was immersed in liquid helium, with the inner-can jacket evacuated to reduce thermal conduction. The temperature of the inner-can bath could be lowered to $\sim$1.2 K with a mechanical pump and measured with a germanium resistor. A pressure regulator and/or an electronic temperature regulator was used to regulate the temperature to better than 1 mK above the λ point and $\sim 100\,\mu$K below.

Low-voltage measurements were done by using a rf SQUID in external feedback mode with a voltage resolution of $\sim$10 pV in a 10-Hz bandwidth. Typical signal voltages across the tunnel junction were less than 100 nV. In our supercurrent effect measurements we fixed the current bias through the junction and measured the reduction in voltage. For the samples reported here, within experimental error, no voltage change was detected across the junction in the absence of a junction bias current with supercurrents up to the critical current.

We expect that the supercurrent density was relatively uniform across the thickness of the films since twice the penetration depth $2\lambda\approx1000$ Å was comparable to or larger than the thickness of the film, $d\sim800$ Å. The order parameter was also uniform since twice the coherence length 2ξ ($\gtrsim$4600 Å in Sn; $\gtrsim$1800 Å in Sn-In) was much larger than d. The uniformity of the current distribution across the width of the films was improved by the presence of the Nb ground plane. Measurements on high-resistance junctions show that the expected nonuniformities have a negligible effect.[2]

IV. EXPERIMENTAL RESULTS AND DISCUSSION

We report results on the five best samples in which we measured the junction resistance as a function of supercurrent. [The "best" samples have the largest increase in $R_j(T)$ at low temperatures.] Table I lists the relevant parameters of the films and junctions. T_c is the transition temperature of the Sn and Sn-In films, which are very close to that of bulk Sn, 3.74 K. $\rho_{4.2\,K}$ and l are the resistivity and the mean free path of the films at 4.2 K, and we used $\rho_{4.2\,K}l = 1.05\times10^{-15}$ Ω m^2 (Ref. 12) to calculate l. w and d are the width and thickness of the films. w_{SiO} is the length of the junction defined by SiO. $I_c(0)$, the ideal critical current at zero temperature, is calculated by using measured dimensions and material parameters and Eq. (14). The normal-state density of states $2N(0)$ is[44] 2.78×10^{28} eV^{-1} m^{-3}.

The following parameters in Table I are determined by fitting the data. R_N is the intrinsic resistance of the junction. τ_{tun}^{-1} is the proximity-effect-induced tunneling rate. $\tau_{e\text{-ph}}(T_c)^{-1}$ is the electron-phonon scattering rate at the Fermi energy at T_c. $\langle a^2\rangle_0$ is the mean-square intrinsic gap-anisotropy parameter for pure, bulk Sn. We used a Fermi velocity of[44] $v_F = 0.65\times10^6$ m s^{-1} for Sn and Sn-In to obtain τ^{-1} from l.

A. Resistance as a function of temperature

Figures 3 and 4 show the normalized junction resistances $R_j(T)/R_N$ versus normalized temperatures T/T_c for samples A13 and D30. Data at lower temperatures are shown in Figs. 5 and 6. The solid curves were calculated using the best-fit parameters from these data and from the supercurrent-effect data discussed below. Also shown on the figures is the equilibrium part of the normalized junction resistance, $R_{eq}(T)/R_N$ (dashed curve).

The measured and calculated junction resistances diverge towards T_c as the charge-imbalance relaxation rate vanishes at T_c.[1–6] As T decreases below T_c, the charge-imbalance component of $R_j(T)$ steady decreases while the equilibrium part increases. At low enough temperatures, the measured resistance falls below the calculated value, presumably because of imperfections in the junction insulator. The junction resistance rises towards lower temperatures because the equilibrium part of the junction resistance depends exponentially on Δ/k_BT at low temperatures.

There are several fitting parameters involved and it is important to see how each is determined. Of course, in

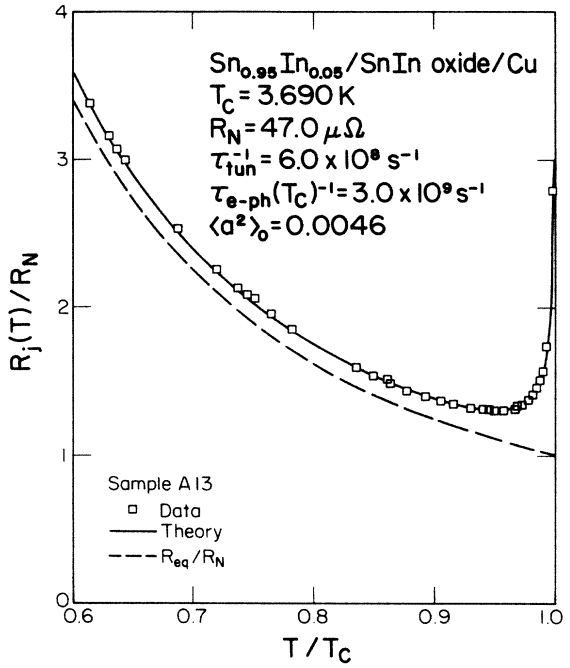

FIG. 3. The normalized junction resistance $R_j(T)/R_N$ vs T/T_c for sample A13 (low-resistance Sn-In junction). The squares are the data and the solid curve is calculated. The resistance diverges toward T_c since the charge-imbalance relaxation rate vanishes towards T_c. Also shown is the theoretical equilibrium part of the junction resistance curve (dashed curve). The difference between the solid curve and the dashed curve is the charge-imbalance part of the junction resistance.

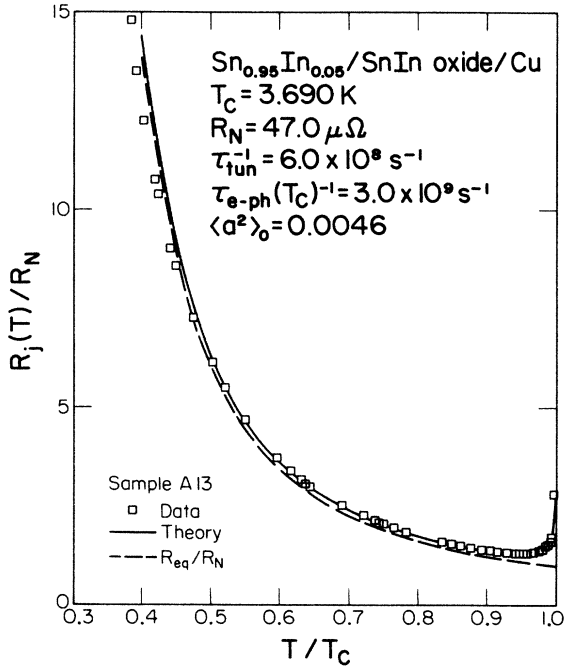

FIG. 5. Low-temperature behavior of sample A13 (low-resistance Sn-In junction). The squares are the data and the solid curve is calculated. The data lie slightly below the theory curve. At $0.4T_c$, the measured normalized resistance is about 10% smaller than the calculated value.

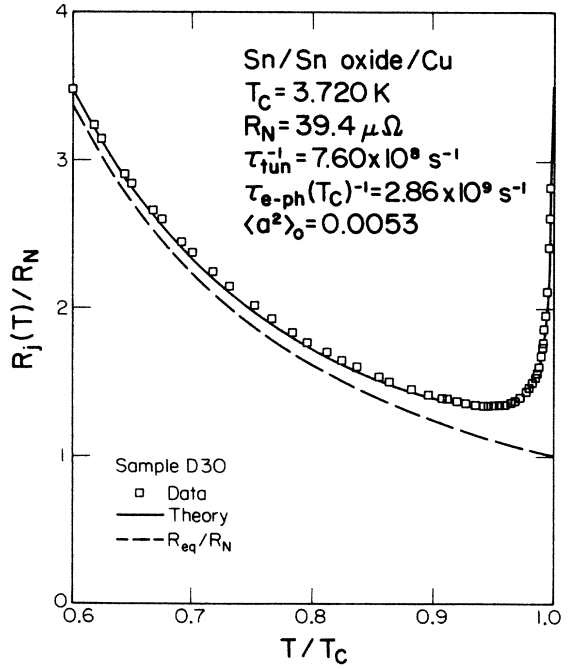

FIG. 4. The normalized junction resistance $R_j(T)/R_N$ vs T/T_c for sample D30 (low-resistance Sn junction). The squares are the data and the solid curve is calculated. The dashed curve is the equilibrium part of the junction resistance. The difference between the solid curve and the dashed curve is the charge-imbalance part of the junction resistance.

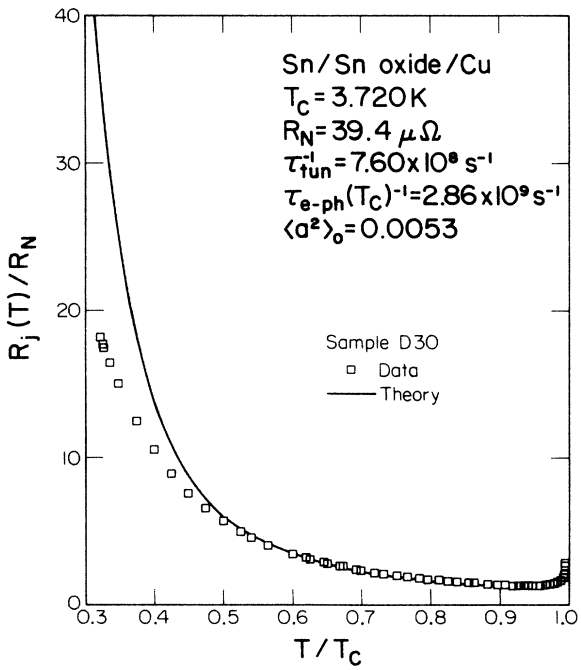

FIG. 6. Low-temperature behavior of sample D30 (low-resistance Sn junction). The squares are the data and the solid curve is calculated. At the lowest temperature the data lie significantly below the theory curve. At $0.4T_c$, the measured normalized resistance is 23% smaller than the calculated value.

the end, all parameters are adjusted to give the best fit to both $R_j(T)$ and $R_j(I_s)$. However, a conceptual picture of which data are most important in determining each parameter is useful and goes as follows. By fitting the $R_j(T)$ versus T data, we obtain values for R_N and for the ratio $\tau_{e\text{-ph}}(T_c)/\tau_{\text{tun}}$ of the tunneling rate τ_{tun}^{-1} and the electron-phonon scattering rate at T_c, $\tau_{e\text{-ph}}(T_c)^{-1}$. [We could use Eq. (4) to calculate $1/\tau_{\text{tun}}$ and then $1/\tau_{e\text{-ph}}(T_c)$ as was done in Ref. 6. Instead, we leave R_N and $1/\tau_{\text{tun}}$ as independent parameters and check Eq. (4) at the end as an internal consistency check.] The absolute values of these rates are determined from $R_j(I_s)$ as described below.

The gap-anisotropy rate cannot be determined from $R_j(T)/R_N$ because it is most important at low temperatures where the charge-imbalance resistance $R_{Q^*}(T)$ is relatively small, and deviations from theory become obvious. Including the gap-anisotropy rate in the fit near T_c gives a fit about as good as with electron-phonon and tunneling relaxation mechanisms only. It reduces the fitted value of $1/\tau_{e\text{-ph}}(T_c)$ by only about 20%. Thus, the gap-anisotropy rate and the magnitude of the tunneling rate, or electron-phonon rate, are essentially the only two parameters available for fitting $R_j(I_s)/R_N$ from $0.4T_c$ to $0.95T_c$.

The transition temperature of the superconductor is determined from strip resistance versus temperature for a bare film deposited at the same time as the base film, so that T_c is not a fitting parameter. Note that the depression in T_c from the proximity-effect coupling[5,6,8] between the normal metal Cu and the superconducting Sn is only about 2 mK, so that the T_c of a bare film is nearly the same as a film in a junction.

B. Resistance as a function of supercurrent

Figures 7–10 show the measured reduction in junction resistances normalized to the junction resistance when there is no supercurrent, $-\delta R_j(T,I_s)/R_j(T,I_s=0)$, versus normalized supercurrent squared, $I_s^2/I_c(0)^2$, together with calculated curves for samples A13 and D30. The data and the theory agree from $\sim 0.5T_c$ to $\sim 0.995T_c$ in both magnitude and temperature dependence. (Data for $T > 0.95T_c$ are not shown here because of drastic change in the scale of current axis. They can be found in Ref. 45.) Note that both the fractional change in R_j and the absolute change, for a given current, vary by large factors over the temperature range studied. Near T_c, the variation is largely from the T dependence of the density of superconducting electrons, $n_s(T)$, but also from the T dependence of the electron-phonon rate. At low temperatures, the variation is from the T dependence of the gap-anisotropy rate and the exponential dependence of the equilibrium resistance $R_{\text{eq}}(T)$ on Δ/k_BT.

The magnitude of $1/\tau_{e\text{-ph}}(T_c)$ is determined from the data near $0.95T_c$ where the gap-anisotropy rate is relatively small. The magnitude of the gap-anisotropy rate is determined at low temperatures where it is the dominant rate. The excellent agreement at intermediate tempera-

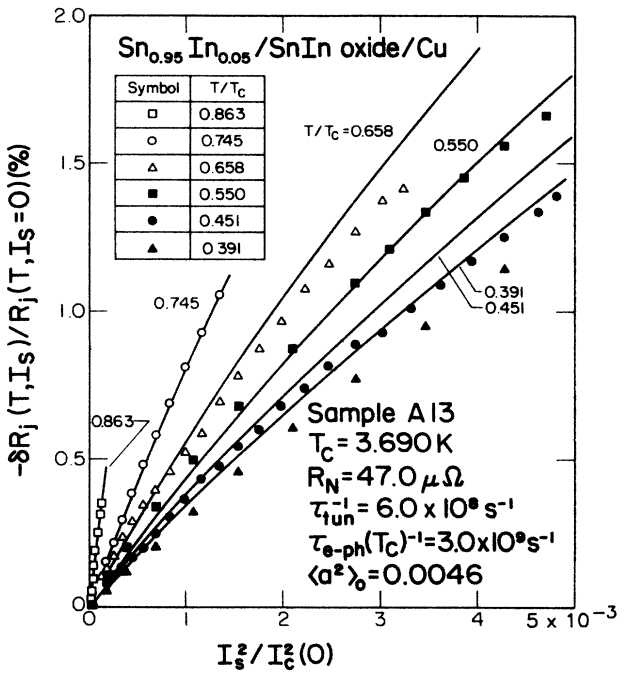

FIG. 7. Reduction in junction resistance normalized to the junction resistance at zero supercurrent, $-\delta R_j(T,I_s)/R_j(T,I_s=0)$, as a function of normalized supercurrent squared, $I_s(T)^2/I_c(0)^2$, for sample A13 (low-resistance Sn-In junction). The solid lines are the theoretical results. The temperature dependence of the data is in excellent agreement with theory over the temperature range $\sim 0.55T_c$ to $\sim 0.95T_c$.

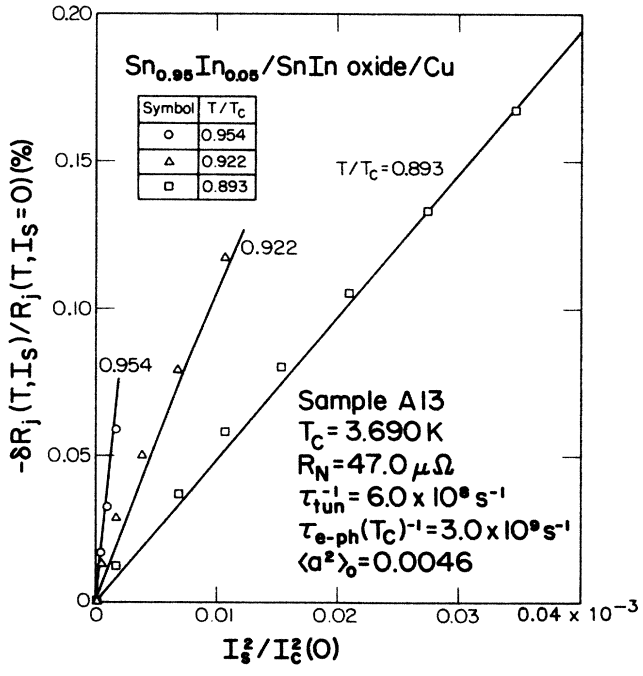

FIG. 8. Same as in Fig. 7, but for T near T_c only. Note changes in scales on both axes.

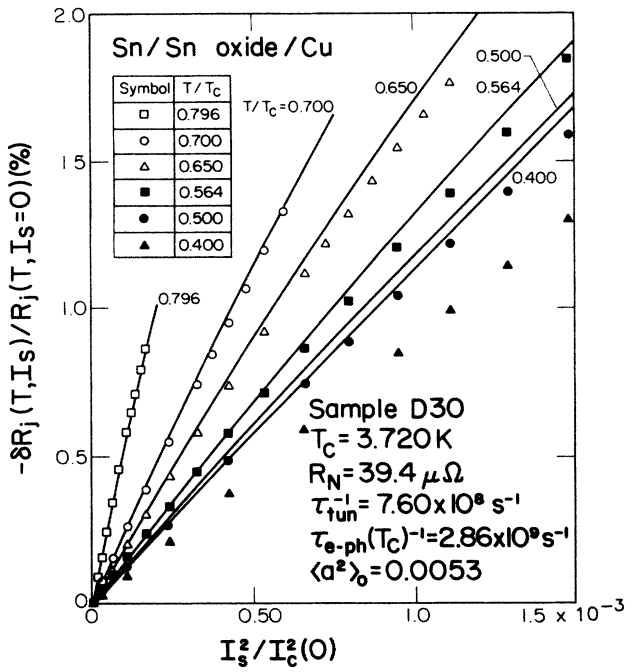

FIG. 9. Reduction in junction resistance normalized to the junction resistance at zero supercurrent, $-\delta R_j(T,I_s)/R_j(T,I_s=0)$, as a function of normalized supercurrent squared, $I_s(T)^2/I_c(0)^2$, for sample D30 (low-resistance Sn junction). The solid lines are the theoretical results. The temperature dependence of the data is in excellent agreement with theory over the temperature range $\sim 0.55T_c$ to $\sim 0.95T_c$.

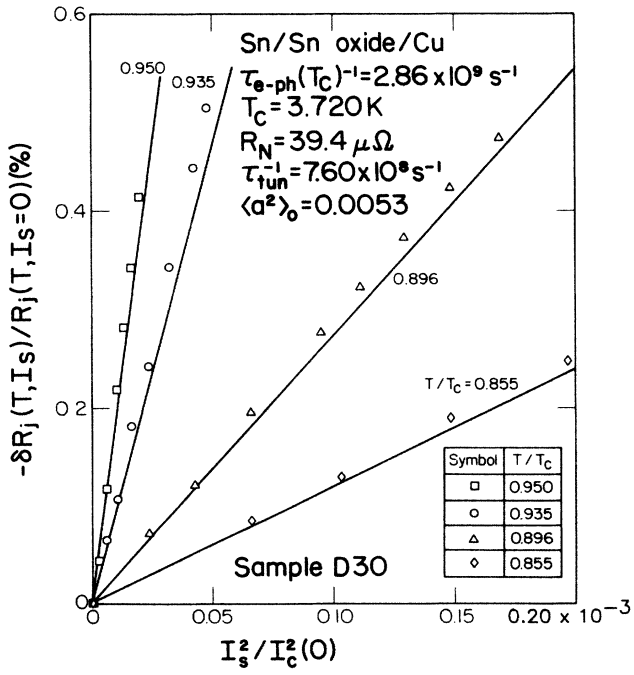

FIG. 10. Same as Fig. 9, but for T near to T_c. Note changes in scales on both axes.

tures is a rigorous test of the theory since there are no more adjustable parameters. The quantitative agreement of the fitted rates with literature values is described in Secs. IV C and IV D.

For temperatures below about $0.5T_c$, data deviate from theory, just as for $R_j(T)$. For sample A13, the temperature dependence of the junction resistance deviates from theory only slightly and the supercurrent effect is only $\sim 10\%$ smaller than the expected value at $T=0.4T_c$. For sample D30, however, the junction resistance data are about 23% low at $T=0.4T_c$ and the supercurrent effect data deviate further from the calculated values.

The $\delta R_j(T,I_s)$-versus-I_s curves we measured were usually symmetric with respect to the $I_s=0$ point. The current bias through the junction was usually negligible compared to the applied supercurrent. However, the point of symmetry occasionally shifted to a different value which was larger than half of the bias current through the junction. We showed data for which the supercurrent was measured with respect to the symmetry point. The largest source of uncertainty is different at different temperatures. In general, the uncertainty in $\delta R_j/R_j$ is less than 10% at all temperatures reported here.

The uncertainties in the scattering rates extracted for sample D30 are about 10% for $\tau_{e\text{-ph}}(T_c)^{-1}$ and 20% for $\langle a^2\rangle_0$. The electron-phonon rate is determined more accurately than the gap-anisotropy parameter because both R_j-versus-T and R_j-versus-I_s data are used to determine the rate. Of course, the uncertainties in the rates extracted are larger for junctions of lower quality because the temperature range in which the data agree with the theory is narrower.

C. Electron-phonon scattering rate

In this section we compare the electron-phonon rate obtained from our measurements with values in the literature. The electron-phonon rate we obtain is the inelastic electron-phonon scattering rate at the Fermi surface at $T=T_c$. Assuming that the electron-phonon coupling function $\alpha^2F(\omega)$ has the usual ω^2 dependence from the Debye density of phonon states, then[14,22]

$$\tau_{e\text{-ph}}(T_c)^{-1}=14\zeta(3)\alpha^2F(k_BT_c)k_BT_c/\hbar\propto T_c^3 \qquad (15)$$

relates our rate to $\alpha^2F(\omega)$. Our value, from Table I, is $(2.8\pm 10\%)\times 10^9\ \mathrm{s}^{-1}$, averaged over all samples of Sn and Sn-In. This value was obtained even for poor-quality junctions by fitting $R_j(T)$ near T_c.

Kaplan[23] have reviewed the literature values of $\alpha^2F(\omega)$ and have calculated that $\tau_{e\text{-ph}}(T_c)^{-1}=3.65\times 10^9\ \mathrm{s}^{-1}$. This is good agreement, considering the uncertainty in determining $\alpha^2F(\omega)$ for low frequency.

Various experimental methods have been used to determine an effective electron-phonon rate in Sn, with results listed in Table II. All methods involve nonequilibrium superconductivity. Only the present work and studies involving the three-film, double-junction configuration[11–14,16,17] involve a time- and space-independent disequilibrium. Because of the physical simplicity, the theory for these experiments is very well developed and straight-

TABLE II. Measurements of the electron-phonon scattering rate in Sn.

Reference	Quantities measured	$\tau_{e\text{-ph}}(T_c)^{-1}(10^9\ s^{-1})$
46	Nonlinearity in flux flow	2.0
47	Nonlinearity in flux flow	2.0
48	Quasiparticle recombination lifetime	≤ 0.1[a]
49	$\delta\mu_p(x)$ in phase-slip center	8.02
50,51	$\delta\mu_p(x)$ in phase-slip center	1.25
12	$\delta\mu_s$ due to Q^*	7.14
15	Sn/Ir/Sn interface resistance	3.85
15	$Sn_{0.99}In_{0.01}$/Ir/$Sn_{0.99}In_{0.01}$ interface resistance	9.09
23	Calculated from theoretical $\alpha^2F(\omega)$	3.65
Present work	R_j vs T and R_j vs I_s for Sn/Sn-oxide/Cu and $Sn_{0.95}In_{0.05}$/Sn-In-oxide/Cu junctions	2.80

[a]Extrapolated from low-temperature recombination-time data.

forward to apply. The electron-phonon rate obtained by Clarke and Paterson, $7.1\times10^9\ s^{-1}$, is rather large. This result may be affected by heating in the injector junction used to generate the charge imbalance measured at the detector.

Musienko, Dmitrenko, and Volotskaya[46] and subsequently Klein *et al.*[47] studied energy relaxation in dynamic mixed states of superconducting Sn and obtained a phenomenological energy-relaxation rate τ_E^{-1} of $2.0\times10^9\ s^{-1}$. Parker and Williams[48] studied energy-gap relaxation under phonon irradiation at low temperatures and obtained an energy-relaxation rate of less than $10^8\ s^{-1}$ for pure Sn when their results were extrapolated to T_c. For both of these experiments, large uncertainties in the relaxation rate arise because of uncertainties in estimating the effective thermal coupling between the samples and the substrate and/or the liquid-helium bath. Thus, the relation between the rate obtained from these measurements and from the present charge-imbalance relaxation measurements is unclear.

Several experiments on phase-slip centers[49–54] have also been used to extract the inelastic scattering rate in Sn. The measured resistance of quasi-one-dimensional films are attributed to normal regions which have a characteristic charge-imbalance decay length Λ. This length is necessary for the normal current to convert into supercurrent or vice versa. The inelastic rates that these authors found for Sn range from 1.2×10^9 to $8\times10^9\ s^{-1}$. The wide range of values probably reflects the large uncertainty from heating in the phase-slip center.

The main difference between our results and those of the earlier three-film, two-junction charge-imbalance technique[12] is in the reproducibility. Perhaps heating complicated the data analysis in the three-film technique because of the high injection current used. Results from previous measurements show a large scatter in the values of the electron-phonon rate. We point out that all the previous results used the measured detector-junction conductance in the calculation of the charge-imbalance relaxation rate. This gives a good fit to the data only very close to T_c. Our technique, although complicated by the occasional poor quality of the junctions, gives consistent results in the electron-phonon rate and the gap-anisotropy rate for similar samples.

Hsiang and Clarke[15] measured the interface resistance of Sn/Ir/Sn and Sn-In/Ir/Sn-In $S/N/S$ sandwiches. They used a phenomenological model to obtain a rate of $3.85\times10^9\ s^{-1}\pm20\%$ for pure Sn and $9.09\times10^9\ s^{-1}\pm6\%$ for $Sn_{0.99}In_{0.01}$. The ranges given represents the variation from sample to sample, not uncertainties in measurement or analysis. The variation with the electron mean free path or In concentration disagrees with our results, although the magnitude of this rate for pure Sn agrees reasonably well with ours. It is difficult to make a close comparison because the theory of S/N interfaces is very difficult and has been worked out accurately only for temperatures very close to T_c.

D. Gap anisotropy

The mean-square anisotropy in the order parameter averaged over the Fermi surface, $\langle a^2\rangle$, depends on the intrinsic anisotropy of pure Sn and on the ratio of the elastic scattering rate to the order parameter, $\Delta(T)$, as in Eq. (9). We characterize our results in terms of the value extrapolated to pure Sn, $\langle a^2\rangle_0$, because it is independent of T and the electron mean free path, and it can be compared with other results in the literature. $\langle a^2\rangle_0$ is determined from fitting $-\delta R_j(T,I_s)/R_j$ versus I_s^2, Figs. 7–10. Note that even our pure Sn films are so close to the dirty limit of Eq. (9), because of electron scattering from the surfaces of the film, that we do not observe the crossover predicted when $\hbar/\tau_1$ is comparable to Δ. However, as noted above, if we use the dirty-limit expression to fit the Sn data, we find a value of $\langle a^2\rangle_0$ that is 20% smaller than the value listed in Table I and which would be quite different from the values obtained from Sn-In.

Values of $\langle a^2\rangle_0$ listed in Table I for three Sn films and two Sn-In films are remarkably consistent, all lying within 13% of the average value 0.0053. To put this in perspective, note that in the only other systematic charge-imbalance study of anisotropy, in Al films by Chi and Clarke,[14] values of $\langle a^2\rangle_0$ differed by up to a factor of 2 for films with the same resistivity. We believe that the essential difference between the Sn and Sn-In films is that the electron mean free path in Sn-In is 5 times shorter than in Sn, since the resistivity is 5 times larger. The In concentration is too small to change other properties,

such as the electron density of states, appreciably. The agreement between the Sn and Sn-In samples verifies the linear dependence of $\langle a^2 \rangle$ on electron mean free path squared in the dirty limit, as predicted by Anderson's averaging effect and expressed in Eq. (10).

It is difficult to compare in detail our value of $\langle a^2 \rangle_0$ with published values on pure bulk Sn because each measurement technique determines a different average of the anisotropy of Δ over the Fermi surface. Markowitz and Kadanoff used measurements of the dependence of T_c on resistivity for a series of Sn-In crystals to obtain $\langle a^2 \rangle_0 = 0.02$. Measurements of the temperature dependence of the deviation of critical magnetic field from the Bardeen-Cooper-Schrieffer (BCS) (Ref. 55) prediction yield $\langle a^2 \rangle_0 = 0.022$.[56] Tunneling into a crystal facet on the Fermi surface yields an anisotropy of Δ of $\sim 20\%$.[57] We conclude that our value of 0.0053 is reasonable, but may be as much as 4 times too small, implying that the factor of 4 in expression Eq. (10) for $\langle a^2 \rangle$ should be as small as 1 in the dirty limit.

Despite this uncertainty, we emphasize that the Anderson averaging model works amazingly well for large reductions in the gap anisotropy. The temperature-dependent gap-anisotropy parameter $\langle a^2 \rangle$ in our Sn-In films is 100–1000 times smaller than $\langle a^2 \rangle_0$. We are unaware of any other experimental technique capable of measuring such small anisotropies.

V. CONCLUSION

Our major qualitative result is verification of the theory of $S/I/N$ tunnel junctions through measurements of the low-voltage resistance of low-resistance Sn/Sn-oxide/Cu and Sn-In/Sn-In–oxide/Cu tunnel junctions as functions of temperature and transport supercurrent. The detailed microscopic theory includes a steady-state, spatially homogeneous charge imbalance in the superconducting film generated by the current used to measure the junction resistance. This is the first charge-imbalance study to obtain detailed agreement between theory and experiment. This success is likely due to the simple experimental configuration, which eliminates heating as a possible source of error.

Our major quantitative results are the electron-phonon rate at the Fermi energy at $T = T_c$, $\tau_{e\text{-ph}}(T_c)^{-1}$, and the intrinsic gap-anisotropy parameter $\langle a^2 \rangle_0$. The electron-phonon rate we obtain for both Sn and Sn-In is 2.8×10^9 $s^{-1} \pm 10\%$, where the range of $\pm 10\%$ represents the variation over three Sn and two Sn-In samples. This value is in reasonable agreement with the theoretical value 3.65×10^9 s^{-1} of Kaplan *et al.*[23] It is in poor agreement with the S/N interface measurements of Hsiang and Clarke,[15] who find a larger value of 3.85×10^9 $s^{-1} \pm 20\%$ for Sn and a much larger value of 9.09×10^9 $s^{-1} \pm 6\%$ for Sn-In. The source of the discrepancy is unknown. A better microscopic theory of S/N interfaces is needed.

The intrinsic gap-anisotropy parameter $\langle a^2 \rangle_0$ for pure bulk Sn, which we obtain from our Sn and Sn-In films, is 0.0053 ± 0.0007. The 13% scatter is remarkably small. This value agrees reasonably well with values in the literature determined by a variety of other methods. We find that the mean-square anisotropy in Δ is proportional to the electron mean free path squared, as expected from the averaging theory of Anderson.[35]

These results establish that we have, for the first time, both a theory and an experimental method based on charge imbalance that are sufficiently well developed that they can be used together as a tool for studying electron-scattering processes in superconductors. The technique is complimentary to other nonequilibrium techniques such as NMR, ultrasonic attenuation, and thermal conductivity in the information it yields.

ACKNOWLEDGMENTS

This material is based on work supported by the National Science Foundation under Grants Nos. DMR-83-00254 and DMR-85-15370. This work was also supported by a Joseph H. Defrees grant from the Research Corporation. One of us (T.R.L.) gratefully acknowledges support from the Alfred P. Sloan Foundation.

*Present address: Intel Corporation, Hillsboro, Oregon 97124.

[1] T. R. Lemberger, Y. Yen, and S. G. Lee, Phys. Rev. B **35**, 6670 (1987).
[2] Y. Yen, S. G. Lee, and T. R. Lemberger, Phys. Rev. B **36**, 8408 (1987).
[3] S. G. Lee and T. R. Lemberger (unpublished).
[4] T. R. Lemberger, Phys. Rev. Lett. **52**, 1029 (1984).
[5] T. R. Lemberger and Y. Yen, Phys. Rev. B **29**, 6384 (1984).
[6] Y. Yen and T. R. Lemberger, in *Proceedings of the 17th International Conference on Low-Temperature Physics—LT-17,* edited by U. Eckern, A. Schmid, W. Weber, and H. Wühl (North-Holland, Amsterdam, 1984), p. 429.
[7] For several reviews and further references, see *Nonequilibrium Superconductivity, Phonons and Kapitza Boundaries,* Vol. B65 of *NATO Advanced Study Institute Series,* edited by K. E. Gray (Plenum, New York, 1981).
[8] T. R. Lemberger, Phys. Rev. B **29**, 4946 (1984).
[9] P. G. de Gennes, Rev. Mod. Phys. **36**, 225 (1964).
[10] W. L. McMillan, Phys. Rev. **175**, 537 (1968).
[11] J. Clarke, Phys. Rev. Lett. **28**, 1363 (1972).
[12] J. Clarke and J. L. Paterson, J. Low Temp. Phys. **15**, 491 (1974).
[13] M. V. Moody and J. L. Paterson, J. Low Temp. Phys. **34**, 83 (1979).
[14] C. C. Chi and J. Clarke, Phys. Rev. B **19**, 4495 (1979); **21**, 333 (1980).
[15] T. Y. Hsiang and J. Clarke, Phys. Rev. B **21**, 945 (1980).
[16] T. R. Lemberger and J. Clarke, Phys. Rev. B **23**, 1088 (1981).
[17] T. R. Lemberger and J. Clarke, Phys. Rev. B **23**, 1100 (1981).
[18] T. R. Lemberger, Phys. Rev. B **24**, 4105 (1981).
[19] T. R. Lemberger, Physica B+C **107B**, 163 (1981).
[20] M. Tinkham and J. Clarke, Phys. Rev. Lett. **28**, 1366 (1972).
[21] M. Tinkham, Phys. Rev. B **6**, 1747 (1972).
[22] A. Schmid and G. Schön, J. Low Temp. **20**, 207 (1975).

[23]S. B. Kaplan, C. C. Chi, D. N. Langenberg, J. J. Chang, S. Jafarey, and D. J. Scalapino, Phys. Rev. B **14**, 4854 (1977).
[24]U. Eckern and G. Schön, J. Low Temp. Phys. **32**, 821 (1978).
[25]C. J. Pethick and H. Smith, Ann. Phys. (N.Y.) **119**, 133 (1979).
[26]J. J. Chang, Phys. Rev. B **19**, 1420 (1979).
[27]J. Clarke, U. Eckern, A. Schmid, G. Schön, and M. Tinkham, Phys. Rev. B **20**, 3933 (1979).
[28]C. J. Pethick and H. Smith, J. Phys. C **13**, 6313 (1980).
[29]J. Beyer-Nielsen, Ph.D. thesis, H. C. Ørsted Institute, 1983 (unpublished).
[30]J. Beyer-Nielsen, J. Rammer, H. Smith, and C. J. Pethick, J. Low Temp. Phys. **46**, 565 (1982).
[31]K. Maki, in *Superconductivity,* edited by R. D. Parks (Dekker, New York, 1969), p. 1037.
[32]See, for example, *Anisotropy Effects in Superconductors,* edited by H. W. Weber (Plenum, New York, 1977).
[33]S. Bermon, University of Illinois, Technical Report No. 1, 1964 (unpublished).
[34]D. Markowitz and L. P. Kadanoff, Phys. Rev. **131**, 563 (1963).
[35]P. W. Anderson, J. Phys. Chem. Solids **11**, 26 (1959).
[36]See, for example, M. Tinkham, *Introduction to Superconductivity* (McGraw-Hill, New York, 1975), p. 117.
[37]In Tinkham's original paper there is a square for the factor in the square brackets. Reference 12 points out that there should not be a square for the factor in the square brackets.
[38]We shall refer to this as Anderson averaging throughout the rest of the paper.
[39]J. Romijn, T. M. Klapwijk, M. J. Renne, and J. E. Mooij, Phys. Rev. B **26**, 3648 (1982).
[40]W. J. Skoçpol, Phys. Rev. B **14**, 1045 (1976).
[41]We thank Dale van Harlingen for pointing this out.
[42]J. Millstein and M. Tinkham, Phys. Rev. **158**, 325 (1967).
[43]J. P. Burger, G. Deutscher, E. Guyon, and A. Martinet, Phys. Rev. **137**, A853 (1965).
[44]C. Kittel, *Introducting to Solid State Physics,* 5th ed. (Wiley, New York, 1976).
[45]Y. Yen, Ph.D. thesis, The Ohio State University, 1987 (unpublished).
[46]L. E. Musienko, I. M. Dmitrenko, and V. G. Volotskaya, Pis'ma Zh. Eksp. Teor. Fiz. **31**, 603 (1980) [JETP Lett. **31**, 567 (1980)].
[47]W. Klein, R. P. Huebener, S. Gauss, and J. Parisi, J. Low Temp. Phys. **61**, 413 (1985).
[48]W. H. Parker and W. D. Williams, Phys. Rev. Lett. **29**, 924 (1972).
[49]G. J. Dolan and L. D. Jackel, Phys. Rev. Lett. **39**, 1628 (1977).
[50]W. J. Skoçpol, M. R. Beasley, and M. Tinkham, J. Low Temp. Phys. **16**, 145 (1974).
[51]A. M. Kadin, L. N. Smith, and W. J. Skoçpol, J. Low Temp. Phys. **38**, 497 (1980).
[52]W. J. Skoçpol, in *Nonequilibrium Superconductivity, Phonons, and Kapitza Boundaries,* Vol. B65 *NATO Advanced Study Institute Series,* edited by K. E. Gray (Plenum, New York, 1981).
[53]W. J, Skoçpol, M. R. Beasley, and M. Tinkham, J. Low Temp. Phys. **16**, 145 (1974).
[54]A. M. Kadin, L. N. Smith, and W. J. Skoçpol J. Low Temp. Phys. **38**, 497 (1980).
[55]J. Bardeen, L. N. Cooper, and J. R. Schrieffer, Phys. Rev. **108**, 1175 (1957).
[56]J. E. Guethes, C. A. Reynolds, and M. A. Mitchell, Phys. Rev. **150**, 346 (1966).
[57]N. V. Zavaritskii, Zh. Eksp. Teor. Fiz. **48**, 837 (1965) [Sov. Phys.—JETP **18**, 1260 (1964)]; [**21**, 557 (1965)].